IAMG'98, Proceedings of The Fourth Annual Conference of the International Association for Mathematical Geology – Part 2, Ed.: A. Buccianti, G. Nardi, and R. Potenza, September 1998, ISBN Vol. 2: 88-900308-2-8, Pages 633–639

Glacial–interglacial sediment modeling and stratigraphic stacking in the North Atlantic

Bernd J. Haupt
Sonderforschungsbereich 313, Universität Kiel, Heinrich–Hecht–Platz 10, 24118 Kiel, Germany

Karl Stattegger
Geologisch–Paläontontologisches Institut, Universität Kiel, Olshausenstr. 40–60, 24118 Kiel, Germany

1. SUMMARY

The 3–D forward sedimentation model SEDLOB (SEDimentation in Large Ocean Basins) is driven by the thermohaline oceanic circulation and used to generate basin–wide glacial and interglacial sedimentation patterns in the northern North Atlantic. In addition, SEDLOB simulates the lateral inflow and outflow of sediment from coastal sources such as rivers, the input of eolian dust, and ice–rafted debris from melting icebergs.

Sediment accumulation is integrated over succeeding cold and warm periods as defined by the high–resolution Plio/Pleistocene sedimentary record. Based on the stratigraphic record, synthetic cross sections and succeeding sequences in a chronostratigraphic time frame are obtained from this climatically forced basin fill covering the last 2.62 million years.

2. MODEL STRATEGY

The large–scale 3–D forward sedimentation model SEDLOB was developed to generate basin–wide glacial and interglacial sedimentation patterns of the northern North Atlantic (NNA) [6]. SEDLOB is coupled to an ocean general circulation model. Given a specific steady state oceanic circulation pattern with its temperature, salinity, and velocity fields and convection depths, it is possible to add sediment of defined physical properties from various sources to the circulating water volumes.

Stratigraphic modeling involves simulation of the geometry and the build–up of sediment sequences incorporating sequence stratigraphic concepts. Sedimentation processes are linked to basin subsidence and often expressed by the diffusion equation. 2–D stratigraphic models generate depositional sequences in a broad range of stratal geometries [e.g. 2].

In our study we model the 3–D sediment transport and sediment accumulation process during the sequence of glacial and interglacial stages from the onset of the northern hemisphere glaciation 2.62 Ma BP until present. We have chosen two time slices as reference sedimentation patterns. The first one is the Modern/Holocene (HM) warm interglacial stage, the second one is the cold last glacial maximum (LGM, 21600 calendar years BP).

The HM experiment is based on the present–day oceanic conditions and climate system [4,5,6]. The currents south of Iceland match with the generalized circulation of bottom water given for the North Atlantic by McCave and Tucholke [10].

For the LGM experiment we use wind forcing from the T42 atmospheric circulation model of Lautenschlager and Herterich [8]. To include the glacial sea–level fall the overall depth was reduced by 100 meters. Shelf glaciation (Laurentide and European ice sheets) was imitated by a cut–off of all regions shallower than 200 meters. Based on the Levitus [9] reconstructions, sea surface salinities were modified in the northern part of the model area

[13]. The CLIMAP [1] summer reconstruction was used to include thermal forcing and ice cover. These LGM sea surface conditions lead to dramatic changes in ocean circulation in the Norwegian–Greenland Seas (NGS) [4]: a southward shift of sea ice cover, a reduction of the subtropical and subpolar gyres, and a weakening of the Gulf Stream and the Labrador Current. In the southern part of the NGS the cyclonic gyre is intensified and strengthened by temperatures around the freezing point and by high salinity values [3]. The bottom currents south of the Greenland–Iceland–Scotland Ridge are still westward directed, but they are somewhat shifted and intensified.

3. RESULTS

3.1 Sediment accumulation patterns

The glacial/interglacial experiments with SEDLOB were initialized with the same sediment properties (sediment sources and sinking velocity of 0.05 cm s-1 [15]). As a sediment source we prescribed a flux of about 1.0x10-13g cm-2s-1 from the eolian sediment [7]. Additionally, we added lateral sediment sources from rivers and coastal melting icebergs [6].

We were able to reconstruct most known large sediment drifts, e. g. south of the Greenland–Scotland Ridge for both time slices, the HM (Figure 1a) and the LGM (Figure 1b). The HM experiment produces more patchy sediment structures while in the LGM experiment the sediment structures are more pronounced extending in an northeast–southwest direction.. The areas with higher sedimentation rates still fit the well–known sediment drifts or a concentration in near shore areas due to river runoff.

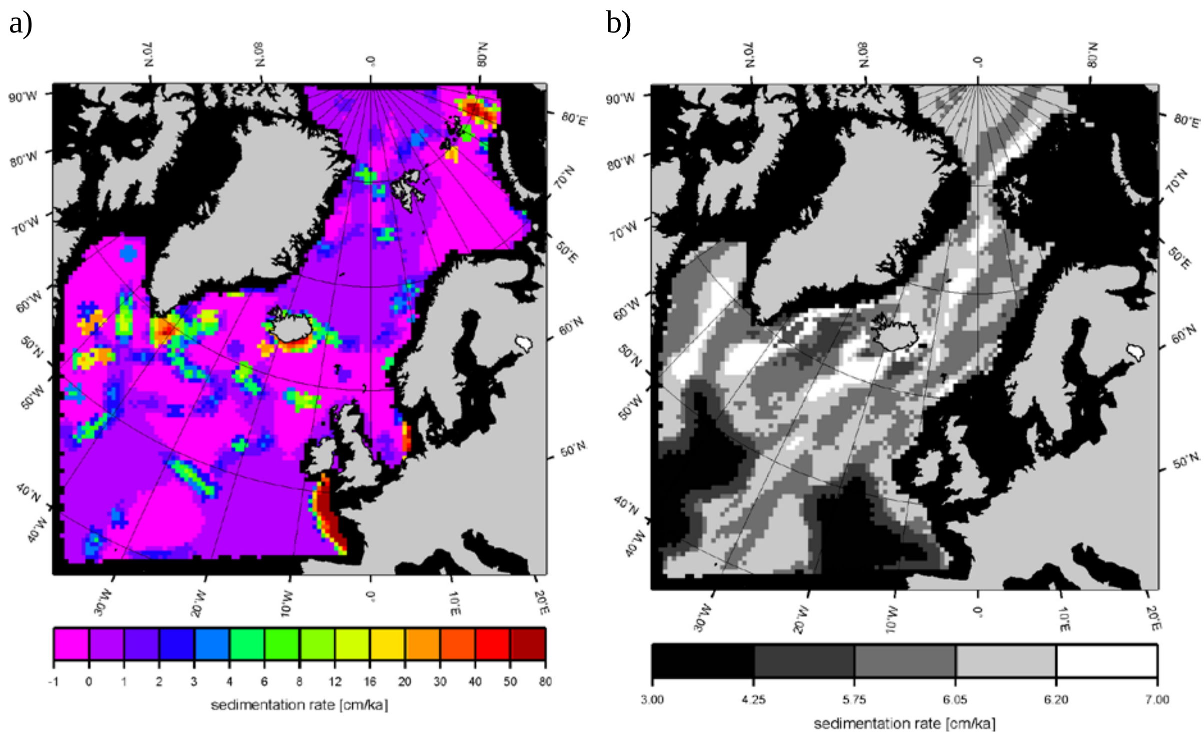

Figure 1: (a) Present–day (HM) and (b) LGM sedimentation rate (centimeters/1000 years).

3.2 Stratigraphic control

North Atlantic site DSDP 607 [12], following the oxygen isotope timescale of Shackleton et al. [14], was used for stratigraphic calibration of glacial and interglacial stages. From the astronomically tuned and globally correlated oxygen isotope record [cf. 16] stages 1 to 104 close to the Matuyama/Gauss magnetic boundary were used, covering the last 2.62 Ma. A continuous time sequence of 33 cold and 34 warm periods was elaborated taking into account shifts in the time dependent mean of oxygen isotope values [11] (Table 1). This glacial/interglacial sequence provides the time frame for the basin fill stacking succeeding cold/warm sedimentation patterns.

Table 1: A continuous time sequence of 33 cold and 34 warm periods covering the last 2.62 Ma years filtered from the North Atlantic site DSDP 607. Only periods with a minimum duration of 15000 years, that will contribute noticeably in the build–up of the sediment column were taken.

climatic period	age in ka	duration in ka
warm	0–16	16
cold	16–113	97
warm	113–143	30
cold	143–194	51
warm	194–223	29
cold	223–294	71
warm	294 –327	33
cold	327–374	47
warm	374–421	47
cold	421–477	56
warm	477–497	20
cold	497–516	19
warm	516–589	73
cold	589–662	73
warm	662–697	35
cold	697–790	93
warm	790–817	27
cold	817–853	36
warm	853–950	97
cold	950–983	33
warm	983–1052	69
cold	1052–1072	20
warm	1072–1128	56

climatic period	age in ka	duration in ka
cold	1128–1159	31
warm	1159–1185	26
cold	1185–1242	57
warm	1242–1259	17
cold	1259–1290	31
warm	1290–1319	29
cold	1319–1336	17
warm	1336–1359	23
cold	1359–1377	18
warm	1377–1396	19
cold	1396–1420	24
warm	1420–1445	25
cold	1445–1468	23
warm	1468–1483	15
cold	1483–1518	35
warm	1518–1538	20
cold	1538–1575	37
warm	1575–1624	49
cold	1624–1655	31
warm	1655–1679	24
cold	1679–1695	16
warm	1695–1729	34
cold	1729–1754	25

climatic period	age in ka	duration in ka
warm	1754–1775	21
cold	1775–1801	26
warm	1801–1917	116
cold	1917–1960	43
warm	1960–1985	25
cold	1985–2006	21
warm	2006–2022	16
cold	2022–2037	15
warm	2037–2092	55
cold	2092–2131	39
warm	2131–2166	35
cold	2166–2191	25
warm	2191–2278	87
cold	2278–2296	18
warm	2296–2424	128
cold	2424–2454	30
warm	2454–2471	17
cold	2471–2525	54
warm	2525–2576	51
cold	2576–2595	19
warm	2595–2620	25

3.3 Stratigraphic simulation and glacial–interglacial stacking pattern

Time–integration and stacking of glacial and interglacial sedimentation patterns results in the climatically forced basin fill of the NNA for the last 2.62 Ma. The initial sediment height at the base 2.62 Ma BP was set to zero. From here we integrated linearly between glacial and interglacial stages to the present (Figure 2).

We are conscious of the fact that using only two climatic stages (interglacial = warm = modern state; glacial = cold = LGM) leads to an oversimplified stratigraphic stacking pattern. Many intermittent periods of “cold” climate over the past 2.6 Ma are significantly different from the LGM. Nevertheless, the modern and the LGM climates are extreme scenarios which are characterized by maximal differences in oceanic circulation and sedimentation.

To elucidate the stratigraphic architecture of this glacial/interglacial basin fill, two characteristic cross sections are examined. The first 3635 kilometer long stratigraphic cross–section A–A’ follows the Greenland–Iceland–Faeroer–Scotland Ridge and continues into the Labrador Sea and is composed of NW–SE and W–E running segments. The second cross–section B–B’ extends over 4689 kilometers in a SW–NE direction from the Mid–Atlantic ridge to the Barents Sea continental margin (see Figure 2 for location).

Cross section A–A’ (Figure 3a) shows a rugged surface. The stratigraphic column is built up to a large extent during glacial periods and slightly eroded during interglacials. The sequence is interrupted by four interglacial high–sedimentation peaks southeast of Greenland. The synthetic stratigraphic section implies high sediment accumulation in certain areas of the Greenland–Iceland–Faeroer–Scotland Ridge building up the well known large sediment drifts that are strongly affected by a remote source of fluvial sediment input. The interglacial sediment oscillations reach several hundreds of meters allowing a maximum sedimentation rate of 30 cm/ka, while the glacial oscillations are reduced by a factor of ten. Cross section B–B’ (Fig. 3b) exhibits a smoother sediment sequence accumulated during glacials with some smaller peaks which developed during interglacials.

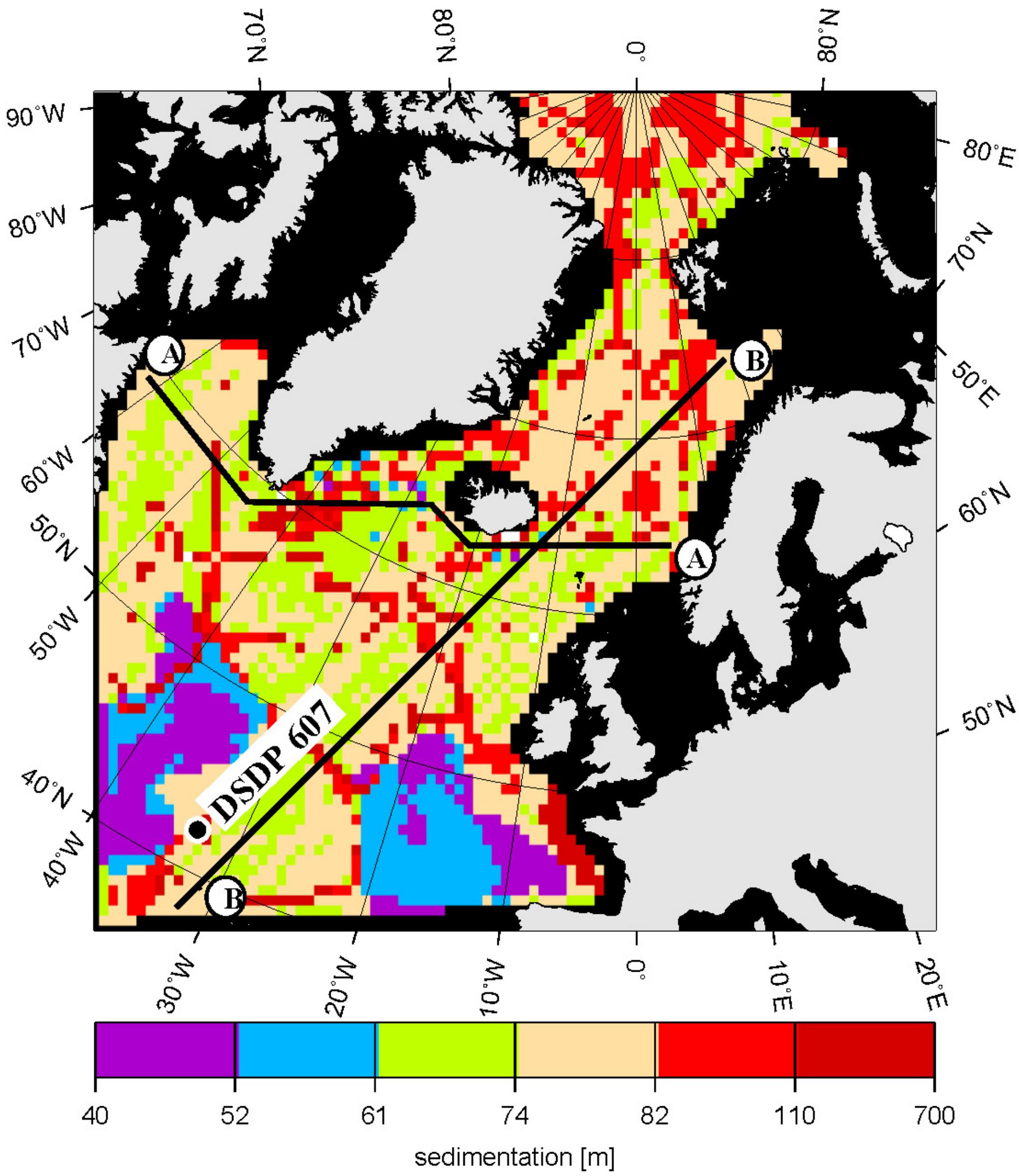

Figure 2: Time–integration and stacking of glacial and interglacial sediment patterns. Additionally the location of the cross–sections A–A' and B–B' (Figure 3), and the location of the site DSDP 607 are shown.

a)

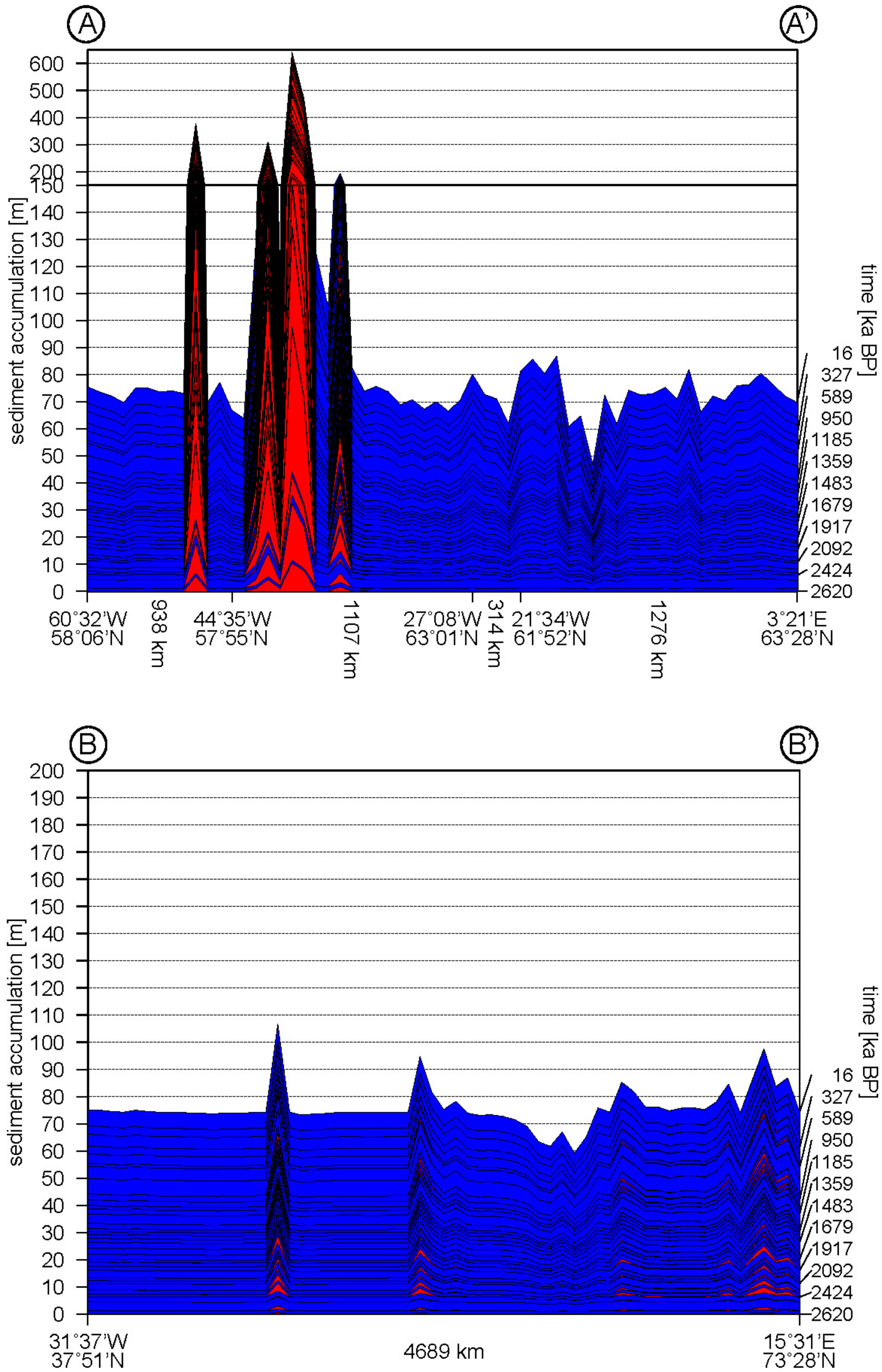

Figure 3: Synthetic stratigraphy (a) along the Greenland–Iceland–Faeroer–Scotland Ridge and (b) from the Mid–Atlantic Ridge to the border of the Barents shelf. The cross–sections A–A' and B–B' are shown in Figure 2.

4. REFERENCES

1. Climate: Long–Range Investigation Mapping and Prediction (CLIMAP) Project Members, 1981, Seasonal reconstructions of the Earth's surface at the Last Glacial Maximum: Boulder, Colorado, Map and Chart Service, Geological Society of America, v. MC–36, p. 1–18.
2. Flemings, P. B., and Grotzinger, J. P., , STRATA — Freeware for analyzing classic stratigraphic problems: GSA Today, 6,12, 1–7 (1996)
3. Haupt, B. J. — Numerische Modellierung der Sedimentation im nördlichen Nordatlantik, v. 54: Germany, University of Kiel, 1995, 129 p.
4. Haupt, B. J., Schäfer–Neth, C., and Stattegger, K. — Modelling Sediment Drifts; A Coupled Oceanic Circulation–Sedimentation Model of the Northern North Atlantic: Paleoceanography, 9/6, 897–916. (1994)
5. Haupt, B. J., Schäfer–Neth, C., and Stattegger, K. — 3–D Numerical Modelling of Late Quaternary Paleoceanography and Sedimentation in the Northern North Atlantic: Geologische Rundschau, 84, 137–150 (1995)
6. Haupt, B. J., Seidov, D., and Stattegger, K. — SEDLOB and PATLOB: Two numerical tools for modeling climatically forced sediment and water volumes transport in large ocean basins, in Stattegger, K. and Harff, J., eds., New York, Springer Verlag, Computerized modeling of sedimentary systems (in press), 1998
7. Honjo, S. — Particle fluxes and modern sedimentation in the polar oceans, Ed. Smith, W. O., eds., Polar Oceanography: San Diego, California, Academic, Part B, 687–739 (1990)
8. Lautenschlager, M., and Herterich, K. — Atmospheric response to ice age conditions — Climatology near the earth's surface: Journal of Geophysical. Research, 95, 22547–22557 (1991)
9. Levitus, S. — Climatological atlas of the world ocean: NOAA Prof. Pap., U.S. Govt. Print. Off., Washington, D.C., 13, 173 p, 1982
10. McCave, I. N., and Tucholke, B. E. — Deep current controlled sedimentation in the western North Atlantic, Ed. Vogt, P. R. and Tucholke, B. E., eds., The Geology of North America, The Western North Atlantic Region: Boulder, Colorado, Geological Society of America, v. M, p. 451–468, 1986
11. Mudelsee, M., and Stattegger, K. — Exploring the structure of the Mid–Pleistocene Revolution with advanced methods of time series analysis, Geologische Rundschau, 86, 499-511 (1997)
12. Raymo, M. E., Ruddiman, W. F., Backman, J., Clement, B. M., and Martinson, D. G. — Late Pliocene variation in northern hemisphere ice–sheets and North Atlantic deep water circulation: Paleoceanography, 4, 413–446 (1989)
13. Seidov, D., Sarnthein, M., Stattegger, K., Prien, R., and Weinelt, M. — Toward a better understanding of the meltwater event near 13.6 ky BP — A numerical modeling approach: Journal of Geophysical Research, 101/C7, 16305–16332 (1994)
14. Shackleton, N. J., Berger, A., and Peltier, W. R. — An alternative astronomical calibration of the lower Pleistocene time scale based on ODP site 677: Trans. R. Soc. Edinburgh Earth Sci., 81, 251–261 (1990)
15. Shanks, A. L., and Trent, J. D. — Marine snow: Sinking rates and potential role in vertical flux: Deep Sea Research, Part A, 27, 137–143 (1980)
16. Tiedemann, R., Sarnthein, M., and Shackleton, N. J. — Astronomic timescale for the Pliocene Atlantic d 18O and dust flux records of Ocean Drilling Program site 659: Paleoceanography, 9, 619–638 (1994)